

Possible origins of defect-induced magnetic ordering in carbon-irradiated graphite

Hosik Lee (이호식)* and Yoshiyuki Miyamoto (宮本良之)

*CREST, Japan Science and Technology Agency, 4-1-8 Honcho, Kawaguchi, Saitama 332-0012, Japan
and Nano Electronics Laboratories, NEC Corporation, 34 Miyukigaoka, Tsukuba, Ibaraki 305-0047, Japan*

Jaejun Yu

*Department of Physics and Astronomy, Center for Strongly Correlated Materials Research, Seoul National University,
Seoul 151-747, Korea*

(Received 19 January 2009; published 31 March 2009)

We investigated possible sources of defect-induced magnetic ordering in carbon-irradiated graphite from first-principles calculations. Among candidate structures with interstitial defect configurations that could be generated during carbon irradiation processes, two metastable configurations with finite magnetic moments were identified. They are coupled ferromagnetically to their neighboring defects, thereby enabling them to contribute to the observed macroscopic magnetic ordering. The Ruderman-Kittel-Kasuya-Yosida interaction is considered as a possible mechanism for the ferromagnetic ordering.

DOI: [10.1103/PhysRevB.79.121404](https://doi.org/10.1103/PhysRevB.79.121404)

PACS number(s): 75.50.Dd, 61.72.jj, 81.05.Uw

Magnetism induced from pure carbon systems has attracted attention due to the absence of localized electrons such as *d* or *f* electrons, which are known to be a source of magnetism in most cases. Magnetic signals from pure carbon systems of pyrolytic carbon were first reported in 1991.¹ More experimental evidence on this topic has been reported during the last decade. Ferromagnetic (FM) hysteresis from amorphouslike carbon² as well as highly oriented pyrolytic graphite³ has been reported, and literature on proton-irradiated graphite^{4,5} supplied convincing evidence for ferromagnetism in pure carbon. Although there remained some skepticism on pure carbon magnetism due to possible contamination from ferromagnetic impurities, successive experiments with reduced and controlled impurity contents have increased confidence in the existence of the observed magnetic properties.⁶⁻⁸

Many theoretical works have suggested possible origins of the magnetism observed in pure carbon systems. These include defect structures such as the peculiar edge state in zigzag edges of graphite,^{9,10} negative Gaussian curvature,¹¹ vacancies,¹² and hydrogen absorption.¹³ Initially, theoretical investigations focused on possible structures and related states as a source of magnetism without considering long-range magnetic ordering. Without the long-range magnetic ordering, it is obvious that only paramagnetic behavior can be observed in any magnetic structure at finite temperature. As for the long-range magnetic ordering, the possibility of two-dimensional (2D) ferromagnetic ordering induced by hydrogen-attached graphene has recently been suggested.¹³ However, no explanation has yet been provided regarding the formation of three-dimensional magnetic ordering.

Recent irradiation experiments have provided clues about the origin of magnetic moments in carbon systems. Irradiating carbon atoms instead of protons has been shown to enhance the observed magnetic signals significantly.⁷ Since the irradiated carbon atoms are likely to form an interstitial-defect structure, one can consider this structure as an origin of the magnetic moments that have been observed in experiments. This type of structure may also explain two different

magnetic moments that show paramagnetic and ferromagnetic signals induced at different transition temperatures.⁶ In that case, the transition temperatures of the paramagnetic and ferromagnetic phases in the experiments were 25 and 350 K, respectively.

This Rapid Communication presents the results of first-principles density-functional calculations for three-dimensional ferromagnetic structures induced by interstitial-defect structures in graphite. Two different types of paramagnetic and ferromagnetic defect structures were found as candidates for the long-range ferromagnetic ordering interactions. These magnetic structures are discussed in connection to the experimental results of two different magnetic origins corresponding to two different transition temperatures.⁶ As mentioned in the previous paragraph, the 25 K paramagnetic and 350 K ferromagnetic phases are related to specific interstitial-defect structures. We show that it is possible to explain the integration of a three-dimensional ferromagnetic structure with the ferromagnetic ordering driving force in terms of the Ruderman-Kittel-Kasuya-Yosida (RKKY) interaction.¹⁴⁻¹⁶

We performed first-principles density-functional calculations with the local spin-density approximation (LSDA) of a Perdew-Zunger parametrization scheme by using the plane-wave self-consistent field (PWSCF) package.¹⁷ The plane-wave kinetic-energy cutoff for the wave functions (charge density) was 544 (4080) eV. The Brillouin-zone integration was performed with a $3 \times 3 \times 3$ Monkhorst-Pack *k*-point grid. We constructed a $5 \times 5 \times 1$ unit cell by extending a conventional hexagonal unit cell that contains four atoms. Four possible configurations for the interstitial structures shown in Fig. 1 were considered for magnetic properties. Atomic geometries were fully relaxed by invoking the Broyden-Fletcher-Goldfarb-Shanno (BFGS) algorithm until the Hellman-Feynman forces were less than 0.013 eV/Å. Nudged elastic band (NEB) calculations were performed to estimate the stability of the configurations.

First, we obtained the first-principles calculation results for the four interstitial-defect configurations. These configura-

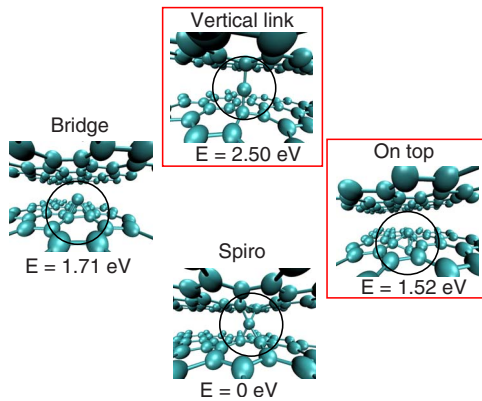


FIG. 1. (Color online) Four interstitial-defect configurations in graphite. Spiro, bridge, on-top, and vertical link structures are shown. Only local structures near the interstitial defects are shown in (black) circles to emphasize them. Configurations in red boxes exhibit magnetic moments. The eV unit shows relative energies to the total energies of the spiro structure.

rations have been considered for the case without magnetism.^{18,19} In this work, we refer to the configurations as “spiro,” “on-top,” “bridge,” and “vertical link” (VL) structures. As Table I shows, our results are quite consistent with those obtained in the previous works in terms of energetics. Further, in our calculations, it is noted that the on-top and VL structures can be magnetically polarized in spin-polarization calculation. The corresponding magnetic moments of the on-top and VL structures are $1.6\mu_B$ and $1.7\mu_B$, respectively.

Spin-density plots in Fig. 2 show magnetic moment distributions. Red (dark gray) balloons in the figure indicate majority spin isosurfaces. The magnetic moment of the on-top structure is distributed only within a single plane indicating that the magnetic state is confined to the 2D layer itself with a very weak interlayer coupling. The same magnetic moment has been also found in the case of single-layer graphene sheets with the defects. Since the magnetic moment is located in a single graphene layer and receives no contribution from any other layers, it is likely to show little correlation with the same type of magnetic moment in other layers.

On the other hand, the magnetic moment in the VL structure in Fig. 2(b) exhibits a distribution for mediation of interlayer interactions. Since the π -state contribution is located in the top and bottom layers evenly, we can expect that it may mediate interlayer correlations. Major and minor spin components of the magnetic moment in the VL structure

TABLE I. Total energy relative to that of lowest-energy configuration, i. e., spiro in eV unit and corresponding magnetic moments in Bohr unit.

	Spiro	Bridge	On top	Vertical link
Li <i>et al.</i> (LDA) (Ref. 18)	0	1.6	1.1	1.5
Ma (GGA) (Ref. 19)	0	1.1	1.1	
Our work (LDA)	0	1.7	1.5	2.5
			($1.6 \mu_B$)	($1.7 \mu_B$)

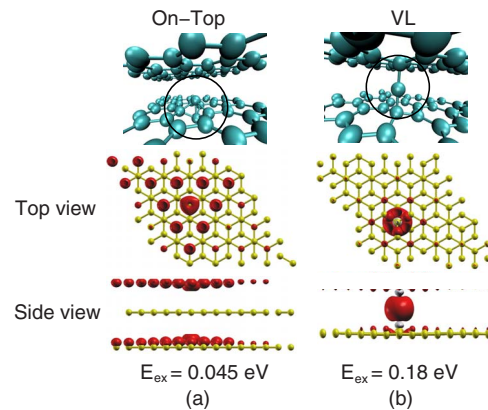


FIG. 2. (Color online) Spin-density plots of paramagnetic and ferromagnetic structures. Red (dark gray) balloons show majority-spin isosurfaces and white (lighter) balloons show minority-spin isosurfaces. The exchange energies at the bottom are defined as spin-unpolarized energy minus spin-polarized energy for the given structures.

come from two unpaired p_x and p_y states and the π state near the Fermi level as shown in Fig. 3. The figure also shows the electronic band structures of majority and minority spins and charge densities. Notably, the localized p_x and p_y states and delocalized conduction-electron π states are identified as the main and minor contributors to the magnetism in the VL structure. The schematic picture in Fig. 3 shows that both the localized and delocalized conduction states contribute to the magnetism of VL structure, indicating possible RKKY interactions. The relevance of the RKKY interaction to the VL structure will be discussed later in this Rapid Communication.

The magnetic moments and exchange energies for the on-top and VL structures are comparable to those previously obtained in experiments.⁶ The exchange energies for the given structures can be obtained by computing the energy difference between the spin-unpolarized and spin-polarized calculations. The corresponding exchange energies for the on-top structure and the VL structure are 0.045 and 0.18 eV, respectively. These values are comparable to the transition temperatures of 25 and 350 K for the paramagnetic and ferromagnetic signals observed in experiments. The qualitative agreement between the results obtained in experiments and those of our calculations implies that magnetism for each of the structures may be related to the paramagnetic or ferromagnetic properties.

In order to investigate the magnetic exchange couplings between the local moments at each defect structure, we carried out the extended LSDA calculations for the two defects in a larger unit cell by varying the distances between the defects. Even for the shortest interaction distance of the second-nearest neighbor, the relative energy of the on-top structure in the FM state is 0.002 eV higher than that of the same structure in the antiferromagnetic (AF) state. When we increase the distance between the defects, the FM and AF energies become degenerate indicating that the magnetic moment in the on-top structure is paramagnetic. Thus, we can conclude that the on-top structure can contribute not to ferromagnetism but to paramagnetism. On the contrary, the

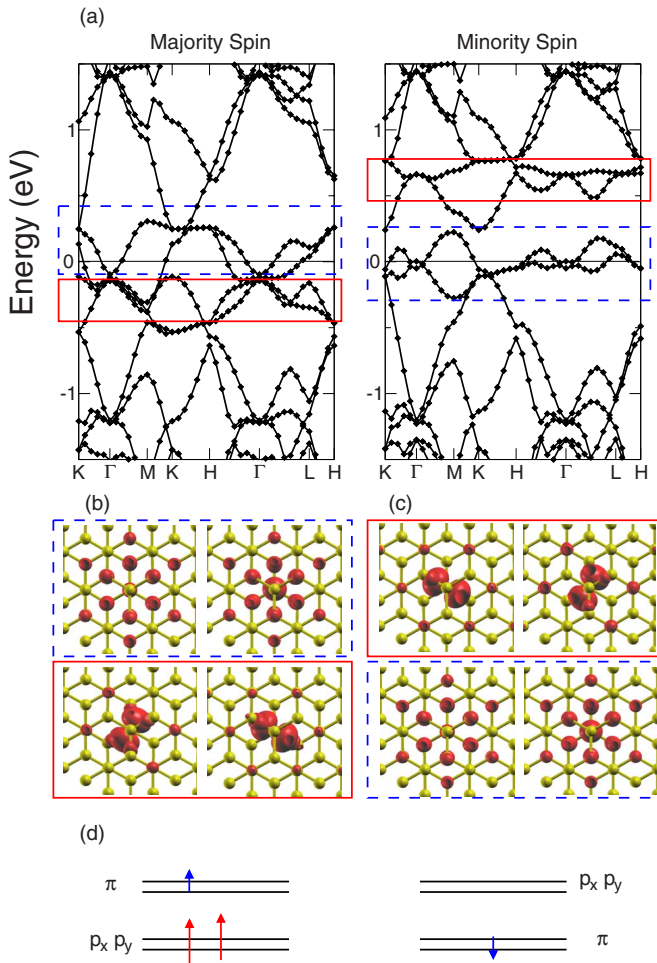


FIG. 3. (Color online) Electronic band structures of majority and minority spins and charge densities. Red (solid) and blue (dashed) rectangles indicate localized unpaired p_x and p_y states and delocalized π states, respectively. (b) and (c) show the charge densities corresponding to the states marked by rectangles in (a) for majority and minority spins, respectively. Schematic of the electronic and the magnetic structures is illustrated in (d).

magnetic moment in the VL structure exhibits stronger ferromagnetic correlations as shown in Figs. 4(a) and 4(b). Figure 4 shows FM and AF spin-density plots and energies relative to the lowest configuration for the VL structures. The FM state is the lower-energy configuration for both the in-plane and the out-of-plane couplings. The energies and spin-density plots of the VL structures clearly indicate the possibility of long-range ferromagnetic ordering. For the out-of-plane configurations, we used two unit cells along the direction perpendicular to the graphite plane as shown in Fig. 4. The reduced energy difference for the FM and AF configurations in the out-of-plane case compared to that for the in-plane case shows that the ferromagnetic correlation for the former is somewhat reduced, but that it still can be sustained with almost the same order of magnitude.

The ferromagnetic coupling between the magnetic defect structures can be explained in terms of the RKKY interactions. The interactions between magnetic impurities in a metallic environment play a crucial role in the ordering of magnetic impurities. As an example, a recent study applying the

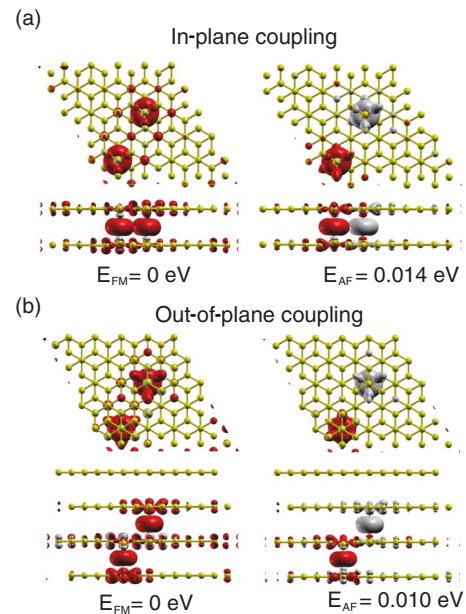


FIG. 4. (Color online) Spin-density plots and corresponding energies of ferro- and antiferromagnetic configurations of the VL structures. Those for the in-plane and out-of-plane orderings are shown in (a) and (b), respectively. The upper and lower parts of each configuration correspond to the top view and side views, respectively. Red (Dark gray) and white (lighter) balloons correspond to the spin-up and spin-down isosurfaces, respectively.

RKKY interaction to a half-filled bipartite graphene lattice concluded that the RKKY interaction between impurities in different and same sublattices shows antiferromagnetic and ferromagnetic correlations, respectively.²⁰ This is consistent with our results on the effect exchange interaction between the defects. The localized p_x and p_y states in the VL structures correspond to the magnetic impurities in the RKKY interactions and the delocalized π state is related to the corresponding conduction states that mediate the RKKY interactions. Unfortunately, the characteristic feature of the RKKY interaction, i.e., the enveloped oscillatory magnetic coupling constant, cannot be estimated in the VL structure since the antiferromagnetic coupling constant is not available due to geometric requirements described below. According to the previous model Hamiltonian calculation results,²⁰ antiferromagnetic coupling appears when the interaction mediates localized magnetic moments located in the different sublattices in the graphite. Only one of the two sublattices can have a VL structure since this structure requires both above and below carbon atoms as shown in Fig. 4(a). Thus, the antiferromagnetic coupling cannot be obtained with the VL structure. Further work is in progress to show the antiferromagnetic coupling which will confirm the RKKY interaction with AA-stacked graphite including four times larger supercell geometry. Our preliminary results are consistent with those of the RKKY model calculation on graphite.²⁰ It contributes to relieving the concern of size effect due to a relatively small supercell used in this work. The details will be published elsewhere.

The contribution of hydrogen to the origin of ferromagnetism in proton-irradiated graphite has been previously

discussed.^{5,7,12,13} Although first-principles calculations have been performed to demonstrate the hydrogen-attached ferromagnetic structure,¹³ the results support only the two-dimensional character of the interactions with almost no coupling structure like the same way as a paramagnetic on-top structure. Moreover, since it does not have the highly localized state needed to sustain the magnetic ordering, the hydrogen-attached structure is less likely to contribute to the ferromagnetism in carbon systems.

To study the stability of the ferromagnetic defect structure, we employed NEB calculations to obtain the energy barriers from VL structures to other structures. From the calculations, the lowest-energy barrier was found to be less than 0.1 eV. In view of experiments where the ferromagnetism was sustained for several months,⁶ the higher-energy barrier is expected. But, the calculated low-energy barrier is suspected to be related to the well-known deficit of local-density approximation (LDA) found at low-density limits.^{21,22} Generally, the breakdown of LDA at low-density limits (e.g., the weak bonding case) is now widely accepted. Since LDA is based on the assumption that electron density is constant or

that it changes very slowly, it can be readily understood that it will fail at a low electron density limit that changes very quickly. In this case, an application of the generalized gradient approximation (GGA) functional does not help much in solving this problem. Recently proposed van der Waals density-functional theory might provide better results.²³

In conclusion, we have shown that the paramagnetic on-top and the ferromagnetic vertical link structures derived from interstitial-defect structures in graphite may be responsible for the ferromagnetic structure which can be extended along both the in-plane and out-of-plane directions, thus resulting in a three-dimensional ferromagnetic structure. Although the energy barrier is small, it is still possible to sustain the ferromagnetic structure. The RKKY interaction is considered to be a driving force for the ferromagnetic ordering.

This work was partially supported by the Korea Science and Engineering Foundation (KOSEF) through the ARP (Grant No. R17-2008-033-01000-0).

*h-lee@cw.jp.nec.com

¹S. Mizogami, M. Mizutani, M. Fukuda, and K. Kawabata, *Synth. Met.* **43**, 3271 (1991).

²K. Murata and H. Ushijima, *J. Appl. Phys.* **79**, 978 (1996).

³P. Esquinazi, A. Setzer, R. Höhne, C. Semmelhack, Y. Kopelevich, D. Spemann, T. Butz, B. Kohlstrunk, and M. Lösche, *Phys. Rev. B* **66**, 024429 (2002).

⁴K.-H. Han, D. Spemann, P. Esquinazi, R. Höhne, V. Riede, and T. Butz, *Adv. Mater. (Weinheim, Ger.)* **15**, 1719 (2003).

⁵P. Esquinazi, D. Spemann, R. Höhne, A. Setzer, K.-H. Han, and T. Butz, *Phys. Rev. Lett.* **91**, 227201 (2003).

⁶J. Barzola-Quiquia, P. Esquinazi, M. Rothermel, D. Spemann, T. Butz, and N. Garcia, *Phys. Rev. B* **76**, 161403(R) (2007).

⁷C. Hwang, S. W. Han, H. Lee, B. C. Lee, B. J. Suh, K. W. Lee, W. Kim, D. Lee, J. S. Park, J. Y. Kim, and Y. P. Lee (unpublished).

⁸H. Ohldag, T. Tylliszczak, R. Höhne, D. Spemann, P. Esquinazi, M. Ungureanu, and T. Butz, *Phys. Rev. Lett.* **98**, 187204 (2007).

⁹M. Fujita, K. Wakabayashi, K. Nakada, and K. Kusakabe, *J. Phys. Soc. Jpn.* **65**, 1920 (1996).

¹⁰H. Lee, Y.-W. Son, N. Park, S. Han, and J. Yu, *Phys. Rev. B* **72**, 174431 (2005).

¹¹N. Park, M. Yoon, S. Berber, J. Ihm, E. Osawa, and D. Tománek, *Phys. Rev. Lett.* **91**, 237204 (2003).

¹²P. O. Lehtinen, A. S. Foster, Y. Ma, A. V. Krasheninnikov, and R. M. Nieminen, *Phys. Rev. Lett.* **93**, 187202 (2004).

¹³O. V. Yazyev and L. Helm, *Phys. Rev. B* **75**, 125408 (2007).

¹⁴M. A. Ruderman and C. Kittel, *Phys. Rev.* **96**, 99 (1954).

¹⁵T. Kasuya, *Prog. Theor. Phys.* **16**, 45 (1956).

¹⁶K. Yosida, *Phys. Rev.* **106**, 893 (1957).

¹⁷S. Baroni, A. Dal Corso, S. De Gironcoli, and P. Giannozzi, <http://www.pwscf.org>

¹⁸L. Li, S. Reich, and J. Robertson, *Phys. Rev. B* **72**, 184109 (2005).

¹⁹Y. Ma, *Phys. Rev. B* **76**, 075419 (2007).

²⁰S. Saremi, *Phys. Rev. B* **76**, 184430 (2007).

²¹B. Hammer, M. Scheffler, K. W. Jacobsen, and J. K. Nørskov, *Phys. Rev. Lett.* **73**, 1400 (1994).

²²J. H. G. Owen, D. R. Bowler, C. M. Goringe, K. Miki, and G. A. D. Briggs, *Phys. Rev. B* **54**, 14153 (1996).

²³H. Rydberg, M. Dion, N. Jacobson, E. Schröder, P. Hyldgaard, S. I. Simak, D. C. Langreth, and B. I. Lundqvist, *Phys. Rev. Lett.* **91**, 126402 (2003).